Available online at www.sciencedirect.com

ScienceDirect

Procedia CIRP 81 (2019) 99–103

www.elsevier.com/locate/procedia

52nd CIRP Conference on Manufacturing Systems

Influence of processing parameters on characteristics of laser-induced periodic surface structures on steel and titanium

Matej Senegačnik[a], Matej Hočevar[b], Peter Gregorčič[a,]*

[a]Faculty of Mechanical Engineering, University of Ljubljana, Aškerčeva 6, 1000 Ljubljana, Slovenia
[b]Institute of Metals and Technology, Lepi pot 11, 1000 Ljubljana, Slovenia

* Corresponding author. Tel.: +386 1 4771 172. *E-mail address:* peter.gregorcic@fs.uni-lj.si

Abstract

Laser-induced periodic surface structures (LIPSS) can appear due to interaction between polarized laser pulses and surface. They can be used to improve or change the surface functionality. Here, titanium and steel surfaces were irradiated by linearly polarized, 30-ps-laser pulses (wavelength of λ=1064 nm) and 45-ns-laser pulses (wavelength of λ=1060 nm), respectively. We investigated how pulse fluence, number of pulses, and pre-existing defects influence LIPSS formation and period. The results show that fluences lower than single-pulse fluence threshold for ablation lead to LIPSS with periods within 150-500 nm, while increased fluence results in larger spatial period between 800-1100 nm. A slight change in processing parameters can also result in different topographical and/or chemical characteristics of the top surface layer, making LIPSS undetectable by SEM.

Keywords: laser surface engineering; laser nanostructuring; LIPSS; laser processing

1. Introduction

In the past decade, laser-induced periodic surface structures (LIPSS) have been a subject of numerous scientific researches due to their promising improvements of surface functionalities [1], such as modification of wettability [2-5], tribological properties [6, 7], wear-resistance [8], and surface colouring [9, 10].

LIPSS is a phenomenon observed upon irradiation of surface by polarized laser pulses. It was first discovered by Birnbaum in 1965 [11], when he irradiated the surface of germanium with fluence near ablation threshold using a ruby laser and noticed formation of periodic structures.

Generally, LIPSS can be categorized into two main groups, depending on the spatial period of the structures Λ [12]. One of the groups is represented by so called *low spatial frequency LIPSS* (LSFL), which form on the surface upon its irradiation with fluence near ablation threshold and usually exhibit spatial periods close to the wavelength (λ) of the incident light ($\Lambda > \lambda/2$) [13]. In this case, the orientation of structures on metal surfaces is perpendicular to the direction of laser beam polarization [14]. The other group of LIPSS exhibits structure orientation either parallel or perpendicular to beam polarization and features periodicity significantly smaller than the irradiation wavelength ($\Lambda << \lambda$), hence the term *high spatial frequency LIPSS* (HSFL) [15]. While LSFL can be produced by various pulse durations ranging from fs pulse range to continuous laser sources with fluence near the ablation threshold [16], formation of HSFL was only reported after irradiation by ultra-short (fs and ps) pulses with fluence below the single-pulse ablation threshold [17]. Other important processing parameters include pulse repetition rate, scanning speed, laser wavelength, angle of incidence and surrounding medium [18, 19].

While the fundamental mechanisms of their formation are still not completely understood and are currently

10.1016/j.procir.2019.03.018

controversially discussed in the literature [20], it is generally accepted that the structures originate from interference of the incident radiation with a surface electromagnetic wave, which is generated at the rough laser ablated surface [21, 22], where the excitation of surface plasmon-polaritons may also play a role. While this model has proven successful in predicting formation of LSFL, some phenomena such as HSFL and multiple bifurcations [23] are difficult to explain using this approach. Therefore, the occurrence of LIPSS has also been explained by J. Reif and his group by developing an alternative model based on self-organisation of the material [23, 24]. This model is very similar to models of surface structuring by ion beam sputtering. It explains a spontaneous formation of surface structures within the laser-modified area by assuming that the absorbed laser energy leads to instabilities of the surface region due to softening and perturbation of crystal binding.

In this work we study the characteristics of LIPSS on titanium and steel surfaces when irradiated by different number of picosecond and nanosecond pulses N_p.

2. Experimental

Single spot experiments were carried out with Nd:YAG laser (Ekspla, Lithuania, PL2250-SH-TH, λ = 1064 nm) delivering linearly polarized 30 ps pulses at λ = 1064 nm with repetition rate of 50 Hz to irradiate polished titanium surfaces in air (Fig. 1). Pulse fluence was varied continuously with an attenuator (A), consisting of a half-wave plate (λ/2) and a linear polarizer (P). Laser spot diameter equalled to approximately 120 µm while pulse energy was measured at 0.23 mJ, resulting in peak fluence of 4 J cm^{-2}. The position of the laser spot on the sample was determined using a laser pointer (LP; λ = 633 nm), deflected off a foldable mirror (FM). Beam expander (BE) was used to widen the beam to a diameter of ~12 mm, before reflecting it off the mirror (M) and focusing it on the sample (S) through a lens (L) with a focal length of 120 mm. Position of the sample was adjusted using a 3D motorized stage (3D MS).

Polished AISI 316L stainless steel surface has also been laser textured using 45 ns laser pulses at λ = 1060 nm emitted from a nanosecond fibre laser (SPI Lasers UK Ltd, United Kingdom, SP-020P-AHS-S-A-Y, λ = 1060 nm). In this case, the laser beam was scanned over the surface with a laser scanning head (Raylase GmbH, Germany, SS-IIE-10). We textured the surface in horizontal parallel lines, separated by 1 µm, with the scanning speed of 1 – 1.55 m s^{-1}, in order to obtain textured surfaces substantially larger (5.0 mm × 2.5 mm)

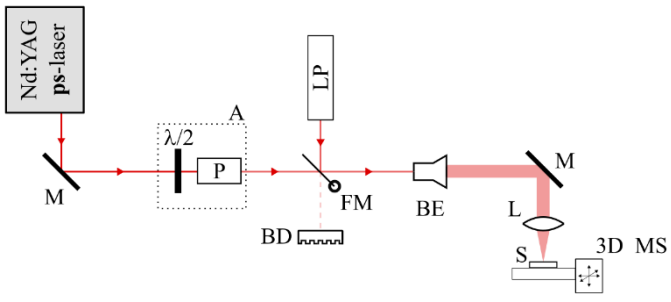

Fig. 1. Experimental setup.

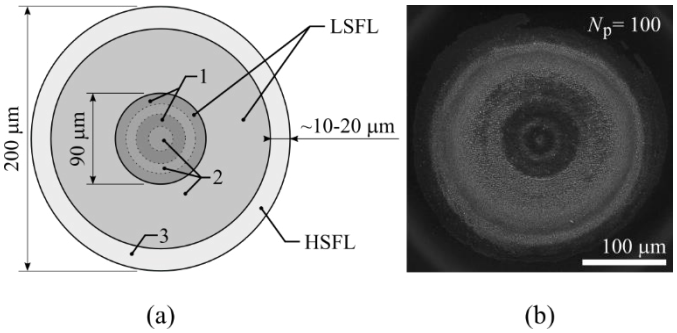

Fig. 2. Typical structures obtained after laser irradiation of titanium depicted (a) schematically and (b) in an SEM micrograph (surface after irradiation with 100 pulses).

than the laser spot diameter (60 µm). During the process, we used an F-Theta lens with a focal length of 163 mm, yielding peak fluence in the focal spot within 1–2 J cm^{-2}. Pulse repetition rate equaled to 100 kHz.

The irradiated surface regions were characterised with an optical microscope (OM) and a scanning electron microscope (SEM) using secondary electron imaging (SEI) and backscattered electron imaging (COMPO) modes.

3. Results and discussion

3.1. Single spot experiments by ps pulses on Ti

Figure 2 shows a spot on the surface with typical LIPSS structures and their dimensions, obtained after irradiating titanium surface. The variance in formed structures is attributed to the spatial fluence profile of the beam, which appears to be of a higher-order Laguerre-Gaussian mode. In the central part of the spot (areas 1 and 2), two distinct types of LSFL with slightly different characteristics appear on the surface in form of circular rings, resembling the local maxima distribution in the fluence profile of the beam. On the outer area of the irradiated spot, where the fluence is lower, HSFL with significantly shorter period is formed.

Formation of LIPSS first begins in the central part of the irradiated spot, at which stage the pre-existing surface defects play an important role. It can be clearly seen from Fig. 3 that

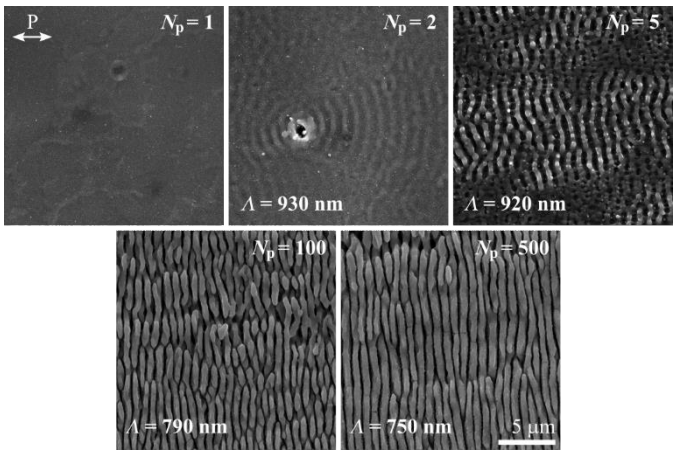

Fig. 3. LSFL evolution with the number of pulses N_p that irradiate titanium surface. The horizontal arrows marked with P indicate the direction of polarization of the beam.

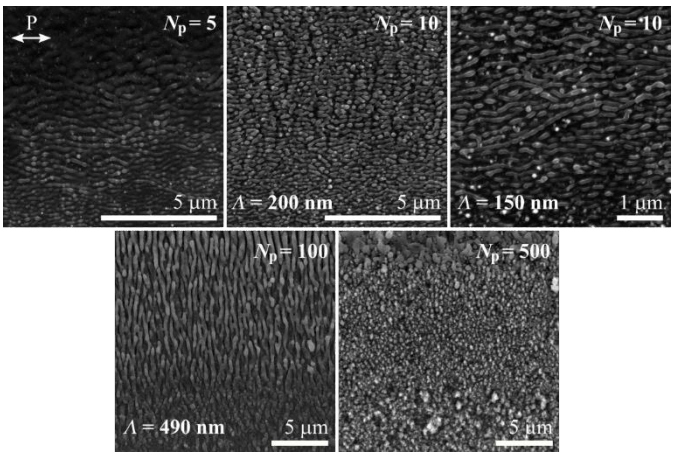

Fig. 4. HSFL obtained at different number of pulses N_p that irradiated the surface. The horizontal arrows marked with P indicate the direction of the polarization of the beam.

LIPSS is more likely to first [after 2 laser pulses (N_p = 2)] appear around an imperfection on the surface, while its orientation at this point in some form correlates to the shape of the imperfection itself. The orientation of structures, however, seems to only follow this trend as long as it remains mainly perpendicular to the direction of polarization of light (indicated by arrows marked with P), which is the orientation of LSFL on metals [15]. Comparable findings have also been reported by Yang *et al.*, who sputtered some silicon nanoparticles on a rough silicon surface before irradiating it with femtosecond laser pulses [25].

Further irradiation by laser pulses causes a more consistent formation of LSFL, regardless of previous defects on the surface. Increasing the number of pulses also deepens the periodic structures, leading to appearance of grooves. Similar observations were reported by Hermens *et al.* in [26] when the surface was processed with either increased pulse fluence or increased number of pulses. The obtained grooves exhibit around 20 % lower spatial period Λ than the LSFL obtained after 2 pulses, as the spatial period was found to monotonically decrease by increasing the number of pulses from 930 nm (first appearance of LSFL after 2 pulses) to 750 nm (after 500 pulses).

In the area 3 in Fig. 2, which is the outer ring of irradiated spot, where fluence decreases below the single pulse ablation threshold, LIPSS with significantly shorter spatial period – HSFL can be observed (Fig. 4), as also shown by Gregorčič *et al.* [20]. These structures require more laser pulses to appear on the surface in comparison to LSFL, while their orientation can be both perpendicular and parallel to the direction of the polarization of light. Spatial period of the obtained HSFL was found to be between 150 nm and 490 nm and could also vary in different areas of the same sample, irradiated with the same number of pulses (in case of 10 pulses).

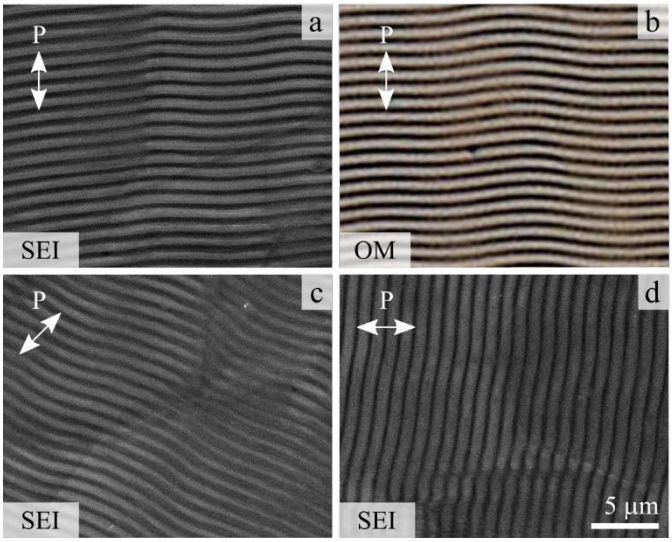

Fig. 5. LSFL achieved by overlapping laser spots on polished steel surface: (a) SEM-SEI and (b) optical-microscope (OM) image of the same surface. (c) and (d) are SEM-SEI images of surfaces obtained by only rotating the direction of polarization of the beam (indicated by arrows marked with P).

3.2. Surface scanning experiments by ns pulses on steel

Overlapping laser spots by choosing appropriate ratio between scanning speed and pulse repetition rate can lead to much larger surface areas covered by LSFL [27]. Fig. 5 shows a collage of micrographs of such surfaces, obtained by scanning the beam at 1 m s^{-1} over 5 mm × 2.5 mm area in horizontal lines, separated by 1 µm. In this case, much longer, 45 ns pulses were used. Pulse fluence equaled to 1 J cm^{-2}. It can be seen that the orientation of LSFL remains perpendicular to the direction of polarization (indicated by arrows marked with P) after its rotation. The structures exhibit a spatial period of 1.0 µm (± 0.05 µm). The ability to see the periodic structures using SEM-SEI also suggests that the observed surface features

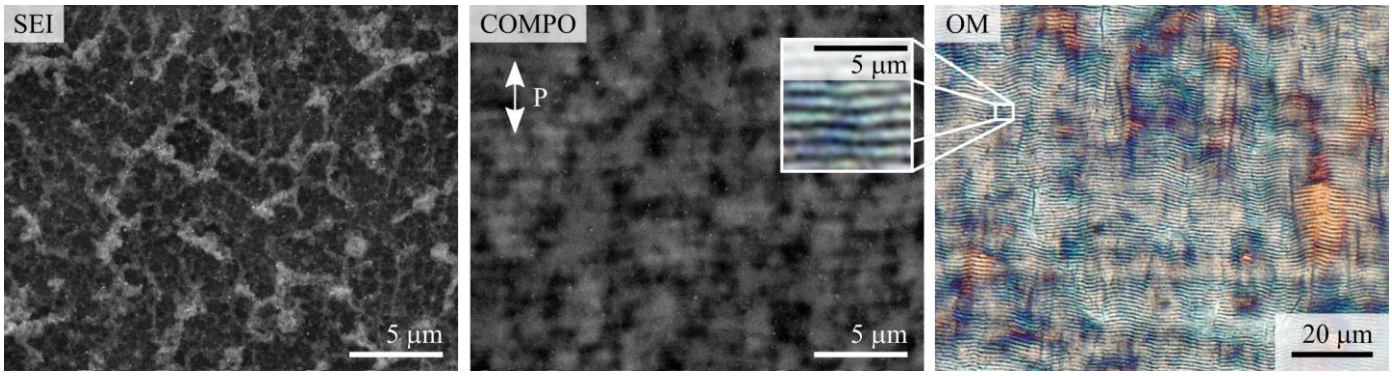

Fig. 6. Micrographs of the same surface, using SEM (SEI and COMPO modes) and an optical microscope (OM). Direction of polarization of light is indicated with arrows marked with P.

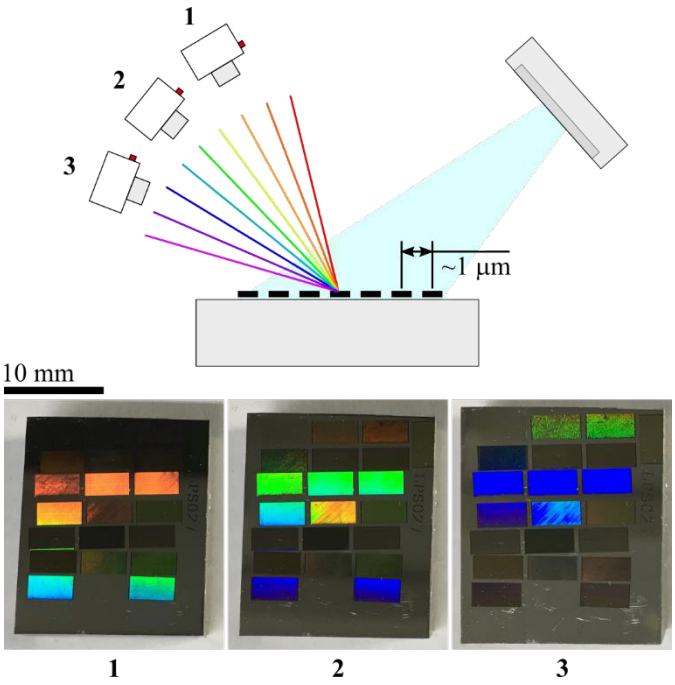

Fig. 7. Changing colour of the surface covered with LSFL when observing from different angles due to diffraction grating effect. Three images (1-3) of the *same* sample surface are taken at different angles of incidence.

a topographical modulation, as opposed to the sample pictured in Fig. 6, where different processing parameters result in the surface covered with LIPSS that can only be detected using an OM. In this case both the pulse fluence and scanning speed were increased (compared to experiments in Fig. 4) from 1 to 2 J cm^{-2} and 1 to 1.55 m s^{-1}, respectively.

Due to laser processing in air atmosphere, the material is covered by a thin oxide layer, whose top surface in this case is presumably flat. LIPSS can therefore not be visible using SEM-SEI by detecting secondary electrons (secondary electron imaging – SEI mode), as this technique forms an image based on topographical modulation of the observed surface. For this reason, the exact same area on the sample was also investigated by observing backscattered electrons emitted from the surface. Since heavy elements (high atomic number) are more likely to backscatter electrons than light elements (low atomic number), they appear brighter in the acquired image and thus enable detection of areas with different chemical compositions (COMPO mode). The resulting image of the surface vaguely shows periodical modulation of composition with the same spatial period as that observed under OM. This can probably be attributed to periodically varying oxide thickness or composition, which result in different amount of oxide backscattered electrons, since the escape depth of backscattered electrons can be greater than the thickness of the oxide. The latter was by Kirner *et al.* reported to exhibit thicknesses of around 200 nm [28].

One of the interesting applications of surfaces covered with LSFL is their changing colour when observing from different angles [10]. As the spatial period of these structures is in the range of wavelength of visible light, the surface acts as a diffraction grating [1]. On a macro scale the effect can be seen as a vivid change in colour of the surface upon its irradiation by a wide spectrum (such as white) light source at different angles of incidence, as shown in Fig. 7. The colours correspond to a palette of "rainbow" colours, similar to which we obtain by refraction of light through a prism.

4. Conclusions

In summary, we presented surface structures that form on titanium and steel when irradiated by polarized laser pulses. When titanium surface was irradiated with picosecond laser pulses, two different types of laser-induced periodic surface structures with different spatial periods appeared on the surface. In the central part of the irradiated spot, where the fluence of the beam is near the threshold for ablation, LSFL with orientation perpendicular to polarization of light appeared on the surface. After first few pulses, its orientation and area of formation were influenced by pre-existing imperfections on the surface. Increasing the number of pulses that irradiate the surface lead to deeper structures (grooves) with decreased spatial period, which was monotonically decreasing for up to 20 % after 500 pulses. On the outer area of irradiated spot, where fluence is below single-shot ablation threshold, HSFL with significantly shorter spatial periods from 150 nm to 500 nm were observed. Their orientation could be both parallel and perpendicular to polarization of light, while their period could vary even when irradiated with the same number of pulses.

Scanning the laser beam with ns pulses across the surface with appropriate overlapping enabled us to obtain LIPSS on greater area. We have shown that the orientation of the structures remains perpendicular to direction of polarization even after its rotation. In some cases the structures were clearly visible by detecting secondary electrons (SEI) using SEM, suggesting topographical modulation of the top surface. However, when processed with slightly different parameters, the produced LIPSS was visible under optical microscope, but could not be observed using SEI. This lead us to believe the top (oxide) surface in this case is flat, while the periodically varying thickness or composition of the oxide on the surface lead to visible periodic "structures".

Acknowledgements

The authors acknowledge the financial support from the Slovenian Research Agency (research core funding Nos. P2-0392 and P2-0132 and project No. Z2-9215) and the support of SPI Lasers Ltd. by loan of their fiber laser within the research project *Surface functionalization by nanosecond fiber laser texturing (nsFLaT)*.

References

[1] J. Reif, Surface Functionalization by Laser-Induced Structuring, in: P.M. Ossi (Ed.) Advances in the Application of Lasers in Materials Science, Springer International Publishing, Cham, 2018, pp. 63-88.
[2] Groenendijk M, Meijer J. Microstructuring using femtosecond pulsed laser ablation. International Congress on Applications of Lasers & Electro-Optics. 2005;18:227-35.
[3] Zorba V, Stratakis E, Barberoglou M, Spanakis E, Tzanetakis P, Fotakis C. Tailoring the wetting response of silicon surfaces via fs laser structuring. Applied Physics A. 2008;93:819-25.
[4] Kietzig A-M, Hatzikiriakos SG, Englezos P. Patterned Superhydrophobic

Metallic Surfaces. Langmuir. 2009;25:4821-7.
[5] Florian C, Skoulas E, Puerto D, Mimidis A, Stratakis E, Solis J, et al. Controlling the Wettability of Steel Surfaces Processed with Femtosecond Laser Pulses. ACS Applied Materials & Interfaces. 2018;10:36564-71.
[6] Mizuno A, Honda T, Kikuchi J, Iwai Y, Yasumaru N, Miyazaki K. Friction Properties of the DLC Film with Periodic Structures in Nano-scale. Tribology Online. 2006;1:44-8.
[7] Yasumaru N, Miyazaki K, Kiuchi J. Control of tribological properties of diamond-like carbon films with femtosecond-laser-induced nanostructuring. Applied Surface Science. 2008;254:2364-8.
[8] Bonse J, Koter R, Hartelt M, Spaltmann D, Pentzien S, Höhm S, et al. Tribological performance of femtosecond laser-induced periodic surface structures on titanium and a high toughness bearing steel. Applied Surface Science. 2015;336:21-7.
[9] Vorobyev AY, Guo C. Colorizing metals with femtosecond laser pulses. Applied Physics Letters. 2008;92:041914.
[10] Dusser B, Sagan Z, Soder H, Faure N, Colombier JP, Jourlin M, et al. Controlled nanostructrures formation by ultra fast laser pulses for color marking. Opt Express. 2010;18:2913-24.
[11] Birnbaum M. Semiconductor Surface Damage Produced by Ruby Lasers. Journal of Applied Physics. 1965;36:3688-9.
[12] Bonse J, Krüger J, Höhm S, Rosenfeld A. Femtosecond laser-induced periodic surface structures. Journal of Laser Applications. 2012;24:042006.
[13] Bonse J, Munz M, Sturm H. Structure formation on the surface of indium phosphide irradiated by femtosecond laser pulses. Journal of Applied Physics. 2004;97:013538.
[14] Bonse J, Rosenfeld A, Krüger J. On the role of surface plasmon polaritons in the formation of laser-induced periodic surface structures upon irradiation of silicon by femtosecond-laser pulses. Journal of Applied Physics. 2009;106:104910.
[15] Bonse J, Höhm S, Kirner SV, Rosenfeld A, Krüger J. Laser-Induced Periodic Surface Structures - A Scientific Evergreen. IEEE Journal of Selected Topics in Quantum Electronics. 2017;23:9000615.
[16] Vorobyev AY, Makin VS, Guo C. Periodic ordering of random surface nanostructures induced by femtosecond laser pulses on metals. Journal of Applied Physics. 2007;101:034903.
[17] Borowiec A, Haugen HK. Subwavelength ripple formation on the surfaces of compound semiconductors irradiated with femtosecond laser pulses. Applied Physics Letters. 2003;82:4462-4.
[18] Maragkaki S, Elkalash A, Gurevich EL. Orientation of ripples induced by ultrafast laser pulses on copper in different liquids. Applied Physics A. 2017;123:721.
[19] Hoppius JS, Maragkaki S, Kanitz A, Gregorčič P, Gurevich EL. Optimization of femtosecond laser processing in liquids. Applied Surface Science. 2019;467-468:255-60.
[20] Gregorčič P, Sedlaček M, Podgornik B, Reif J. Formation of laser-induced periodic surface structures (LIPSS) on tool steel by multiple picosecond laser pulses of different polarizations. Applied Surface Science. 2016;387:698-706.
[21] Bonse J, Krüger J. Pulse number dependence of laser-induced periodic surface structures for femtosecond laser irradiation of silicon. Journal of Applied Physics. 2010;108:034903.
[22] Huang M, Zhao F, Cheng Y, Xu N, Xu Z. Origin of Laser-Induced Near-Subwavelength Ripples: Interference between Surface Plasmons and Incident Laser. ACS Nano. 2009;3:4062-70.
[23] Varlamova O, Reif J, Varlamov S, Bestehorn M. Self-organized surface patterns originating from laser-induced instability. Progress in nonlinear nano-optics: Springer; 2015. p. 3-29.
[24] Varlamova O, Costache F, Reif J, Bestehorn M. Self-organized pattern formation upon femtosecond laser ablation by circularly polarized light. Applied Surface Science. 2006;252:4702-6.
[25] Yang M, Wu Q, Chen Z, Zhang B, Tang B, Yao J, et al. Generation and erasure of femtosecond laser-induced periodic surface structures on nanoparticle-covered silicon by a single laser pulse. Opt Lett. 2014;39:343-6.
[26] Hermens U, Kirner SV, Emonts C, Comanns P, Skoulas E, Mimidis A, et al. Mimicking lizard-like surface structures upon ultrashort laser pulse irradiation of inorganic materials. Applied Surface Science. 2017;418:499-507.
[27] Reif J, Martens C, Uhlig S, Ratzke M, Varlamova O, Valette S, et al. On large area LIPSS coverage by multiple pulses. Applied Surface Science. 2015;336:249-54.
[28] Kirner SV, Wirth T, Sturm H, Krüger J, Bonse J. Nanometer-resolved chemical analyses of femtosecond laser-induced periodic surface structures on titanium. Journal of Applied Physics. 2017;122:104901.